

Poly-energetic Reconstructions in X-ray CT Scanners

V.S. Venumadhav Vedula¹, Nitin Jain², K. Muralidhar², Prabhat Munshi², S. Lukose³,
M.P. Subrananian³ and C. Muralidhar³

¹Presently with GE Bangalore

²Nuclear Engineering & Technology Programme, Indian Institute of Technology,
Kanpur-208 016

³Non-Destructive Evaluation Division, Defence Research and Development Laboratory,
Hyderabad
e-mail: pmunshi@iitk.ac.in

Abstract

Beam-hardening is an artifact, which produces false integrals if polychromatic x-ray sources are used. It is due to the photon energy dependence of the attenuation coefficient. The present work proposes an algorithm for beam-hardening correction incorporating the inherent error formula developed at IIT Kanpur. The effect of beam hardening and its removal along with inherent error is shown on both simulated and experimental data set. It is compared from the point-of-view of nearness of the corrected polychromatic projection data to the desired monochromatic projection data. The results indicate that the algorithm, proposed originally for medical applications, is giving encouraging results for non-medical objects though the physical situations are vastly different.

Keywords: *Tomography, Beam-hardening, Inherent error*

1. Introduction

Tomography has become a routine part in medicine and its use in nondestructive evaluation is increasing day by day. Measurement in x-ray tomography can only be used to estimate the line integrals of the absorption coefficient of photons. Inaccuracies in these estimates are due to width of the x-ray beam, hardening of the beam and photon statistics. When x-rays are passed through an object, their attenuation depends on the density distribution and energy spectrum of the beam. As a consequence of polychromatic x-ray source, the attenuation is no longer a linear function of absorber thickness. The attenuation at a fixed point is generally greater for photons of lower energy and thus energy spectrum of x-rays hardens as it passes through the

material. X-ray beams reaching at particular point inside the material from different directions are likely to have different spectra and therefore these rays attenuate differently at that point and it becomes difficult to interpret image quantitatively. Beam hardening effect has to be compensated to prevent reconstructed image from corruption by cupping artifacts [1-3].

In the present study Convolution Back Projection (CBP) is used for the reconstruction of the projection data and with any filter function in CBP will lead to inherent error in the reconstruction process [4,5]. In the present work, corrections for the cupping artifact and the reduction of the inherent error in the images are discussed.

2. Theory

2.1 Beam Hardening (BH) Correction

The linear x-ray coefficient at a point inside a cross section of the object depends on the position of the point (x, y) and on energy e . It can be denoted as $\mu(x, y, e)$. In case of monochromatic beam it can be written as

$$m_L = \int_L \mu(x, y, e) dl \quad (1)$$

In case of polychromatic beam result will not be m_L but rather an estimate for the more complicated integral

$$P_L = -\ln \int_0^\infty \tau(e) \exp\left(-\int_L \mu(x, y, e) dl\right) de \quad (2)$$

Where $\tau(e)$ is the probability that the detected photon is at energy e [2]. It is assumed that the spectrum of the x-ray beam can be approximated by a discrete spectrum consisting of J energies $e(1), e(2), \dots, e(J)$ and that $e(j)$ is the probability that a detected photon is at energy $e(j)$. Let us divide the cross section into I pixels. We try to estimate the linear attenuation coefficient in each of the I pixels. Thus we can get the discretized version of (1 and 2)

$$m = \sum_{i=1}^I \mu_e^i Z^i \quad (3)$$

$$p = -\ln \sum_{j=1}^J \tau_{e(j)} \exp\left[-\sum_{i=1}^I \mu_{e(j)}^i Z^i\right] \quad (4)$$

The least expensive type of the beam hardening correction can be done by using a function f , which is such that, for source/detector pair $f(p)$ is a reasonable estimate of m . Let us refer to the reconstruction from the so corrected

polychromatic data $\{f(p)\}$ as the first reconstruction. It is a set of I numbers μ_e^i , representing the estimated linear attenuation coefficient at energy \bar{e} of the material in the i th of a total of I pixels.

We see that \bar{m} approximate to m , and \bar{p} approximate to p and hence $f(\bar{p})$ approximate to $f(p)$. Furthermore, since the line integrals in equations (1 and 2) are approximated in the same way in Eqs. (3 and 4), it appears likely that the errors, $\bar{m} - m$ and $f(\bar{p}) - f(p)$ will be similar, i.e. the difference between these errors will be considerably smaller than either of these errors. The term, $\bar{m} - f(\bar{p}) + f(p)$, is an approximation to m and is superior to the use of just $f(p)$. This is true in the sense that

$$\Delta(\{f(p) + \bar{m} - f(\bar{p})\}, \{m\}) < \Delta(\{f(p)\}, \{m\})$$

Where Δ represents the root mean square error. The second reconstruction is one obtained from the data $\bar{m} - f(\bar{p}) + f(p)$. Since the second reconstruction is presumably more accurate than the first one, this process can be repeated [6,7].

2.2 Inherent Error Correction

Projection data obtained from the final iteration of BH correction is free from beam hardening artifacts can be further processed to reduce inherent error. First Kanpur Theorem (KT-1) is applied to remove inherent error caused by filter function [4-5].

Initially factor η is calculated using following equation.

$$\eta = \frac{NMAX1}{NMAX2}$$

Poly-energetic Reconstructions

Where $NMAX1$ and $NMAX2$ are maximum gray level values of monoenergetic and BH corrected data respectively. KT-1 is used to modify the convolving function by the factor η after that final reconstruction is done using modified convolving function.

Beam hardening and inherent error correction is summarized in a combined numerical algorithm as stated below:

1. Reconstruct the polyenergetic projection data of test phantom using CBP. The function f_i is estimated with respect to this specimen, which forms our initial guess O^0 .
2. Collecting a new set of relevant information including geometry, size of specimen from the reconstructed image and coefficients of linear attenuation for the particular materials used, generate specimens X_i at different energies from the x-ray source spectrum.
3. From the generated specimens X_i , evaluate pseudo monochromatic ray sums \bar{m}_i from the equation given below:

$$\bar{m} = \sum_{i=1}^I \mu_{\bar{e}}^i z^i$$

4. Generate pseudo polychromatic ray sum, \bar{p} using equation given below with $\tau_{e(j)}$ as the probability that a detected photon of the x-ray beam is at energy $e(j)$. $\tau_{e(j)}$ can be calculated from the x-ray source spectrum.

$$\bar{p} = -\ln \int_0^E \tau_e \exp \left[-\int_0^D \mu_e(z) dz \right] de$$

5. Get the correlation functions f_i 's, utilizing curve fitting strategy between \bar{m}_i and \bar{p} . The most inexpensive curve-

fitting route is to adopt a polynomial function for f , and determine its coefficients, by least squares technique. f_i 's can be obtained by,

$$\bar{m}_i \approx f_i(\bar{p})$$

$$\bar{m}_i = a_0 + a_1 \bar{p} + a_2 \bar{p}^2 + a_3 \bar{p}^3 + \dots$$

6. Apply correlation function f_i to the actual measured data p recorded in the experiment.

$$m_i \approx f_i(p)$$

7. For the second step of BH correction, a more superior function is given below where the R.M.S. error is minimized.

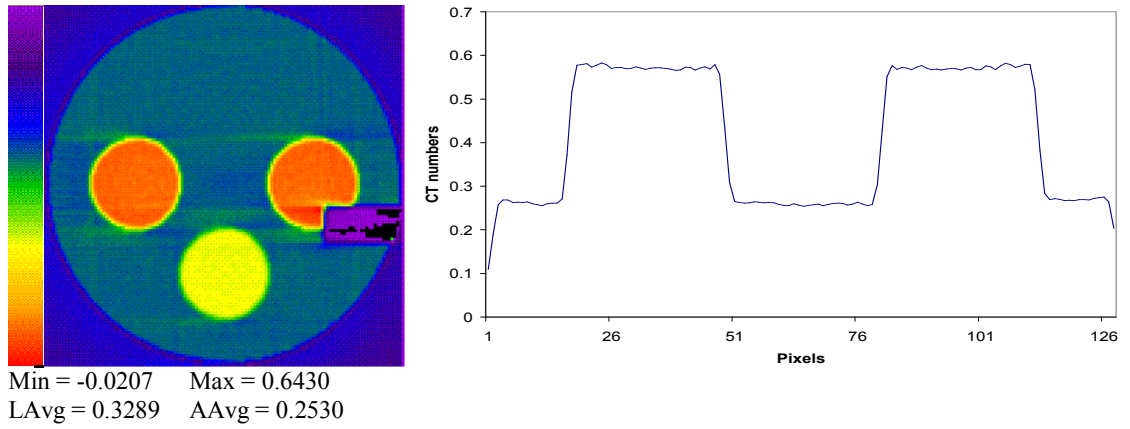
$$m_i = \bar{m}_i - f_i(\bar{p}) + f_i(p)$$

8. Reconstruct m_i obtained from above step and compare with the initial guess O^0 . Improve the initial guess from m_i and repeat above steps till cupping artifact and dark bands are reduced considerably. This completes the BH correction.

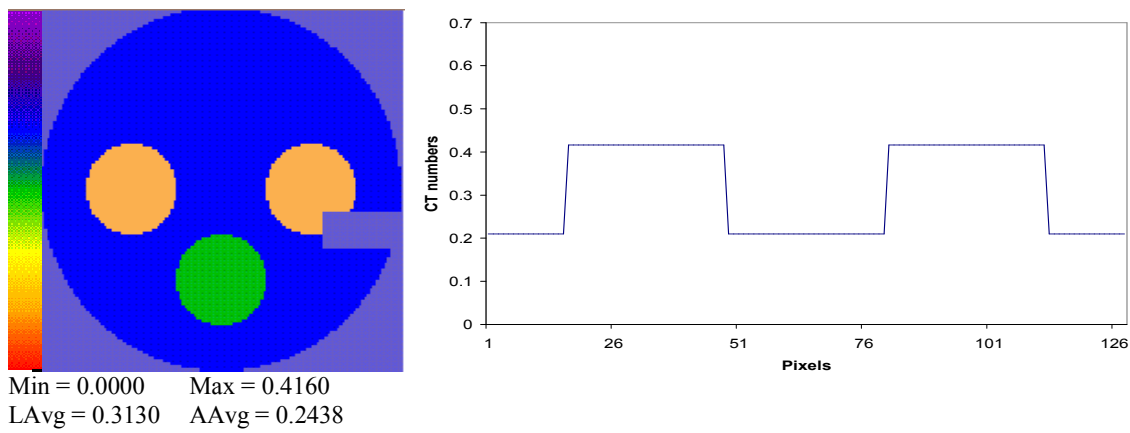
9. Calculate factor η , given by the equation below.

$$\eta = \frac{NMAX1}{NMAX2}$$

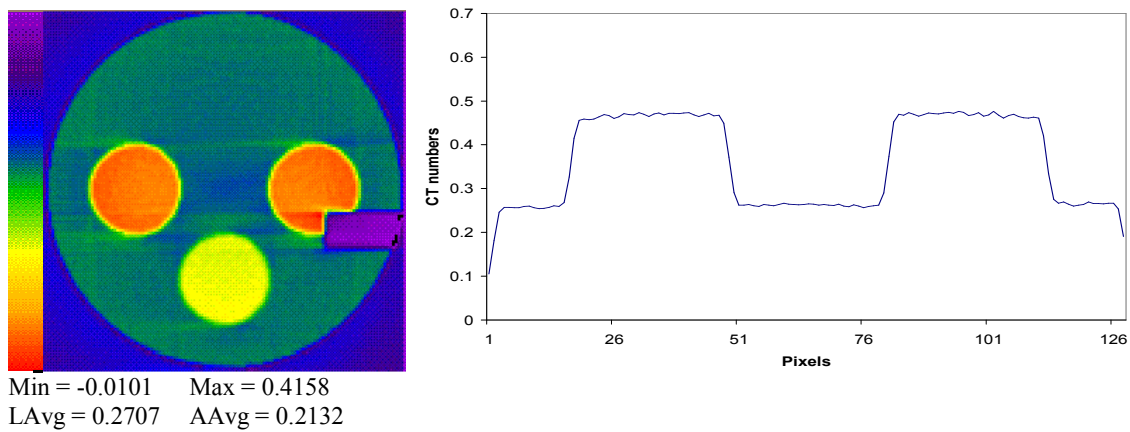
10. Using KT-1, modify the convolving function (here H54) used in CBP algorithm by the factor η . Now reconstruct all the ' m_i 's using this modified filter function. This completes the inherent error correction.



(a)



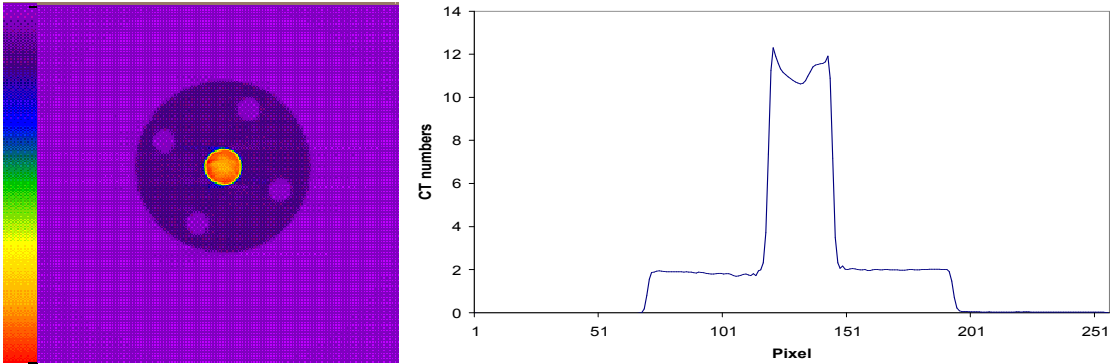
(b)



(c)

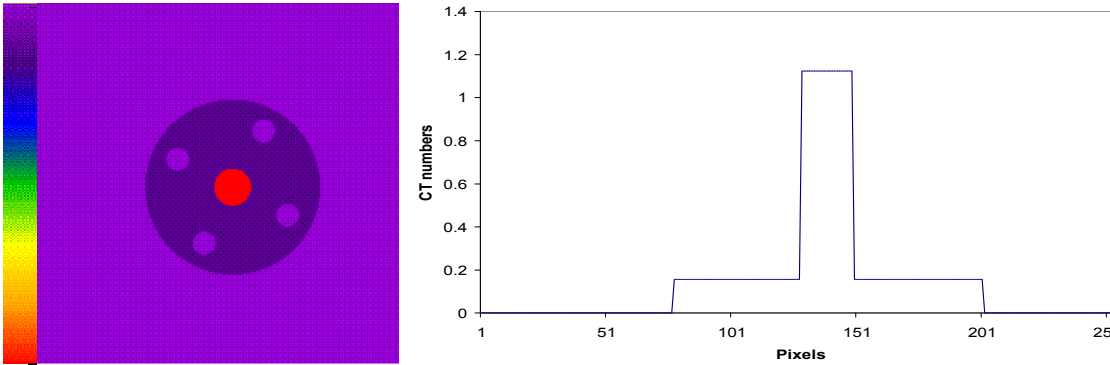
Fig. 1: (a) Polyenergetic reconstruction of simulated specimen (S1) (b) Monoenergetic reconstruction of simulated specimen at 60Kev (c) BH corrected data after applying KT-1 for simulated specimen

Poly-energetic Reconstructions



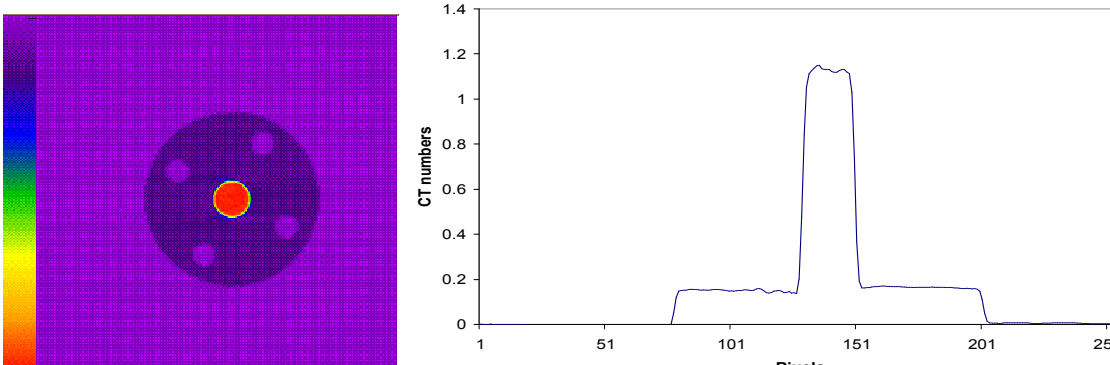
Min = 0.1823 Max = 13.1032
 LAvg = 1.2887 AAvg = 0.6568

(a)



Min = 0.0000 Max = 1.1242
 LAvg = 0.1742 AAvg = 0.0550

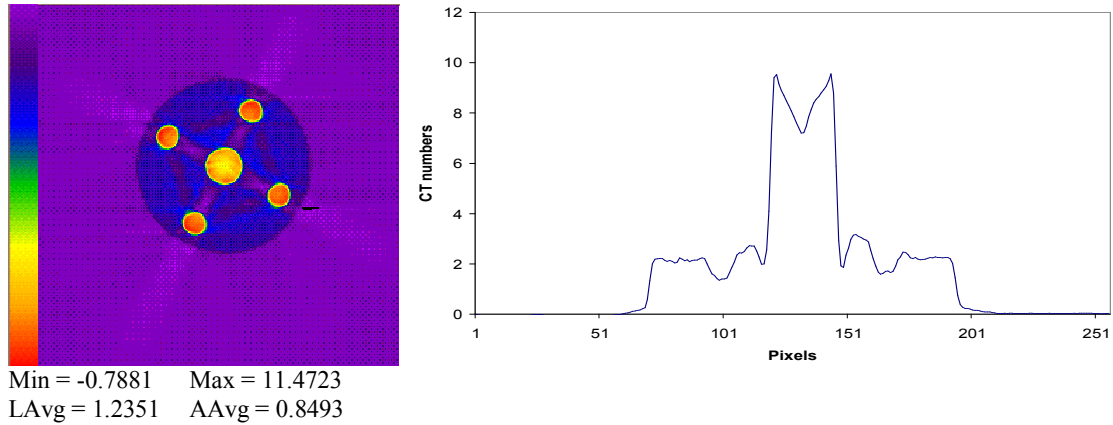
(b)



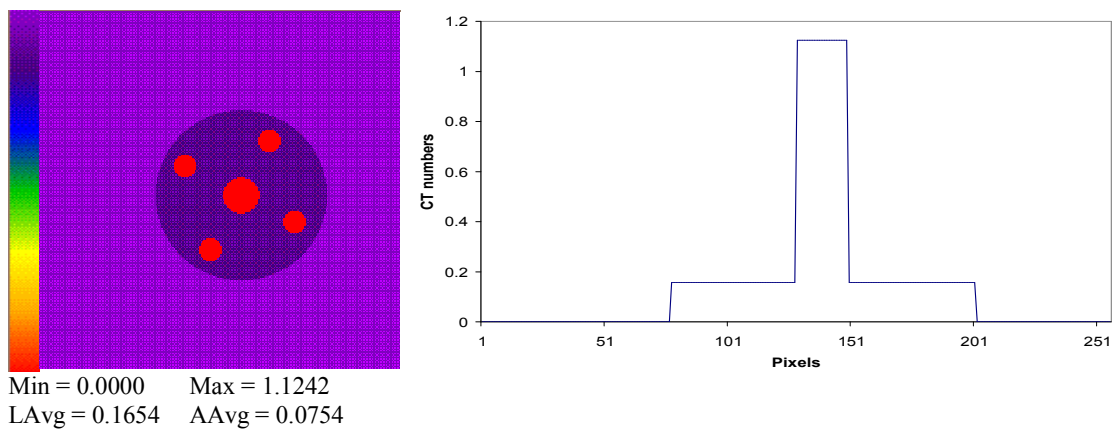
Min = -0.0161 Max = 1.1243
 LAvg = 0.1679 AAvg = 0.0537

(c)

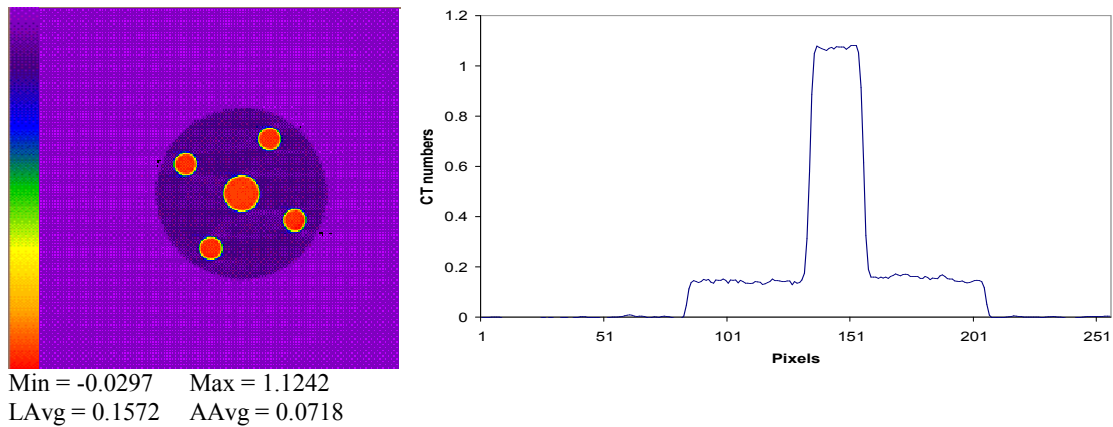
Fig. 2: (a) Polyenergetic reconstruction of specimen-S2 (b) Monoenergetic reconstruction of specimen-S2 at 200Kev (c) Reconstruction of BH corrected data after applying KT-1 for specimen-S2



(a)



(b)



(c)

Fig. 3: (a) Polyenergetic reconstruction of specimen-S3 (b) Monoenergetic reconstruction of specimen-S3 at 200Kev (c) Reconstruction of BH corrected data after applying KT-1 for specimen-S3

3. Specimens Details

a) Specimen-1 (S1):

This is computer generated specimen which contains materials of three different densities. The object considered is a circle made up of material 'a' with three circular holes, one filled with material 'b' and two filled with material 'c'. A crack (of density zero) is introduced in the right inner circular hole with material 'c'.

b) Specimen-2 (S2):

The test phantom considered here is a Perspex cylinder of 60 mm radius with five holes embedded in it. There is a central hole of 12.5mm radius and the remaining four holes each of 7.5 mm radius are placed on either side of the central hole perpendicularly. Here the central hole is filled with a uniform mild steel cylinder and the remaining four holes are unfilled.

c) Specimen-3 (S3):

The test phantom considered here is same as the specimen-2 but with all the holes filled with mild steel. Thus here it is a Perspex cylinder with five mild steel pins embedded in it. Since there is lot of attenuation for this specimen, high energy X-rays should be used for scanning. This specimen is chosen to check for cupping artifact along with dark bands in between the steel pins.

4. Results

Beam Hardening and Inherent error correction has been applied to three specimens. Projection data is acquired in fan beam mode at DRDL Hyderabad, with source to center distance of 1320.7 mm for 512 views and 256 rays for the specimens 2-3. Fan beam projection data is converted to parallel beam mode. X-ray source spectrum is discretised into five energy levels and the probabilities for each of the energy levels are calculated.

Monoenergetic data sets for the above specimens are simulated at the discrete energy levels. The filter function used in all the reconstructions of CBP is Hamming 54, that resolves well the smooth variations in the attenuation coefficient and hence the density. Figures 1-3 show the monoenergetic; polyenergetic and BH corrected images after applying KT-1 theorem with corresponding density profiles for the specimens S1-S3 respectively. Results are given in the above section for all the specimens. Since simulated specimen is generated for 128 rays, it is reconstructed for a grid size of 128. Similarly, specimens S2 and S3 are reconstructed for the grid size of 256. Density profiles are drawn for the specimens for CT numbers versus the pixel numbers. Beam hardening correction is done by fitting second order polynomial in the least squares sense.

5. Discussion

Investigating above results it is depicted that all the polyenergetic reconstructions have high *NMAX* values compared to their corresponding monoenergetic ones. Monoenergetic projections having high probability are considered to give better solutions for beam-hardening correction. Hence, all the monoenergetic reconstructions considered for least squares curve fitting (BH correction) are at the mean energy level. Simulation of the polyenergetic reconstructions should be done with good accuracy to ensure better BH correction, deviation of which may lead to distorted images.

It can be noticed from figures 1-3 that images almost match with the monoenergetic ones and cupping artifact reduces considerably at the final iteration. Fig. 2 shows that BH corrected data of specimen S2 is well approximated to its monoenergetic data. This indicates that algorithm works equally well for object with more than two materials. Dark bands forming bridges between steel pins are

clearly visible from Fig. 3(b), polyenergetic image of specimen S3. Removal of dark bands at the final iteration for specimen S3 can be noticed. Thus algorithm is checked for all the specimens.

Table-1 gives the error estimates for the simulated and experimental specimens at each iteration of the beam hardening correction algorithm, before and after applying inherent error correction. The error presented here is the relative error and should approach zero for the ideal case. It can be observed that error in the images is limiting towards zero after processing them for inherent error correction.

Table 1: Relative errors in the images

Specimen	Error in Polyenergetic data		Error in 2 nd BH iteration	
	Before KT-1	After KT-1	Before KT-1	After KT-1
S1	0.3530	0.2393	0.2801	0.0139
S2	0.9020	0.8972	0.0471	0.00003
S3	0.9142	0.9120	0.0246	0.0004

6. Conclusions

Algorithm works well for both homogenous and heterogeneous cross-sections. For objects with high density materials, cupping artifact and dark bands appeared in the polyenergetic reconstruction can also be reduced to a great extent. First Kanpur error theorem efficiently reduced inherent errors and technique used for these error removal is quite encouraging, applying which

the *NMAX* values for experimental and monoenergetic data are in well agreement. Inherent error for real data is dominated by other experimental errors and there is only 4%-6% of change in relative error after applying KT-1. Numerical algorithm has been checked for all the complexities of beam-hardening, inherent error and different geometries. The proposed algorithm found to be quite robust and is working efficiently for the simulated and experimental data.

7. References

1. Herman G. T., "Correction for Beam Hardening in Computed Tomography", Phys. Med. Biol. 24, 81-106, (1979).
2. Herman G. T., Image Reconstruction from Projections: The Fundamentals of Computerized Tomography, Academic Publishers New York (1980).
3. Herman G. T., and Trivedi S. S., "A Comparative Study of Two Post reconstruction Beam Hardening Correction Methods". IEEE Trans. Med. Imaging, MI-2(3), (1983).
4. Munshi P., "Error Analysis of Tomographic Filters I": Theory, NDT & E International 25(4/5), 191-194, (1992).
5. Munshi P., Rathore R. K. S., Ram K. S. and Kalra M. S., "Error Analysis of Tomographic Filters II": Results, NDT & E International, 26(5), 235-240, (1993).
6. Ramakrishna K., Muralidhar K., Munshi P., "Beam Hardening in Simulated X-ray Tomography", NDT&E international, 39(6), 449-457 (2006).
7. Manzoor M. F., Yadav P., Muralidhar K. and Munshi P., "Image reconstruction of simulated specimens using convolution back projection", Defense Science Journal, 51(2), 175-187, (2001).